Adaptation of the vertical upflow phase map of Wirth to fluidized dense phase conveying of Geldart A powders and validation of the transition boundaries by Eulerian modelling with MFiX-TFM

Prabu Balasubramanian, Andrew Cowell, Don McGlinchey

School of Computing, Engineering and Built Environment
Glasgow Caledonian University, United Kingdom

NETL 2024 Workshop on Multiphase Flow Science, Aug 13-14, 2024
Version-1, 12 Aug 2024

Outline

- Fluidized Dense Phase Conveying
- Vertical upflow phase map
- Proposed (provisional) correlation for the Upper transport velocity (V_{tr2})
- Validation by Eulerian modelling
  - ➢ Powder characteristics
  - ➢ Modelling options
  - ➢ Challenges in model validation
  - ➢ FF – DSU boundary at gross upflow
  - ➢ DSU – dilute phase boundary
  - ➢ Packing limit
- Conclusions

Graphical Abstract

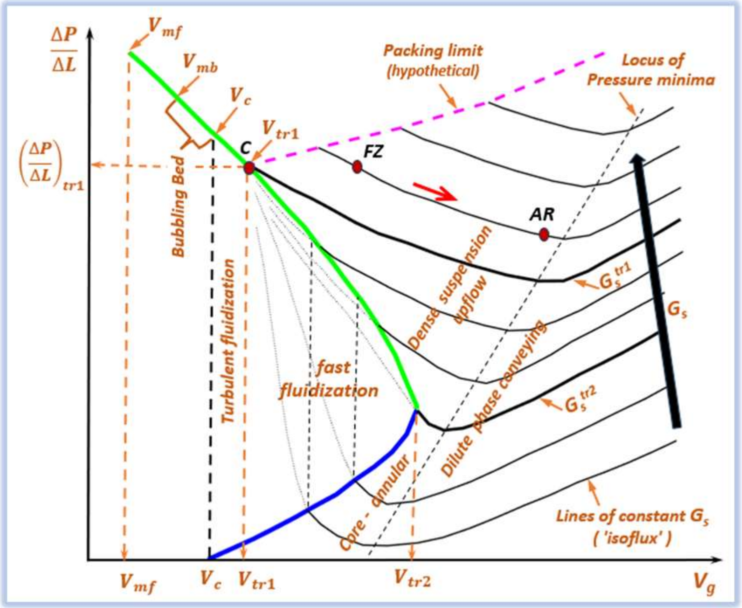

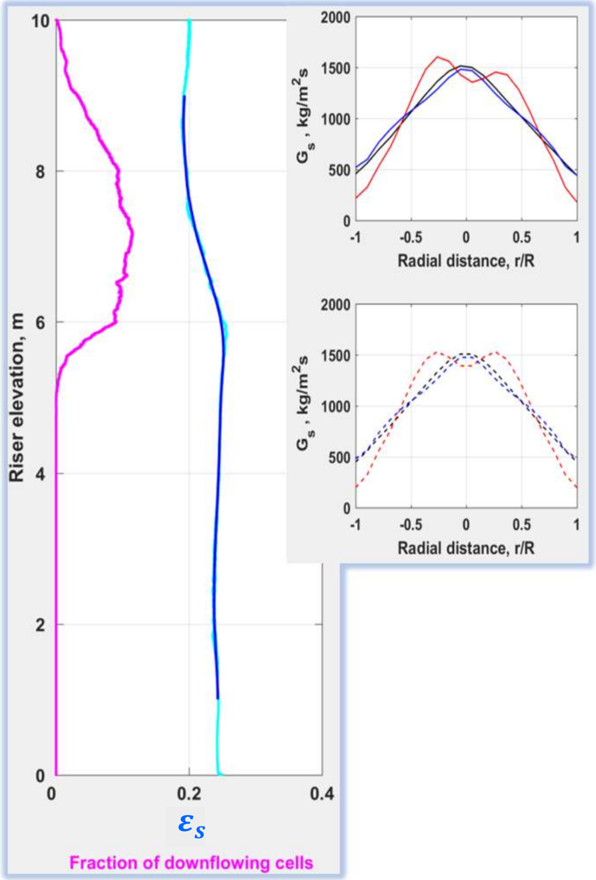

$$Re_{p,tr2} = 3.00\ Ar^{0.80}$$

Fluidized Dense Phase Conveying (FDC)

Fluidized dense phase conveying (FDC)

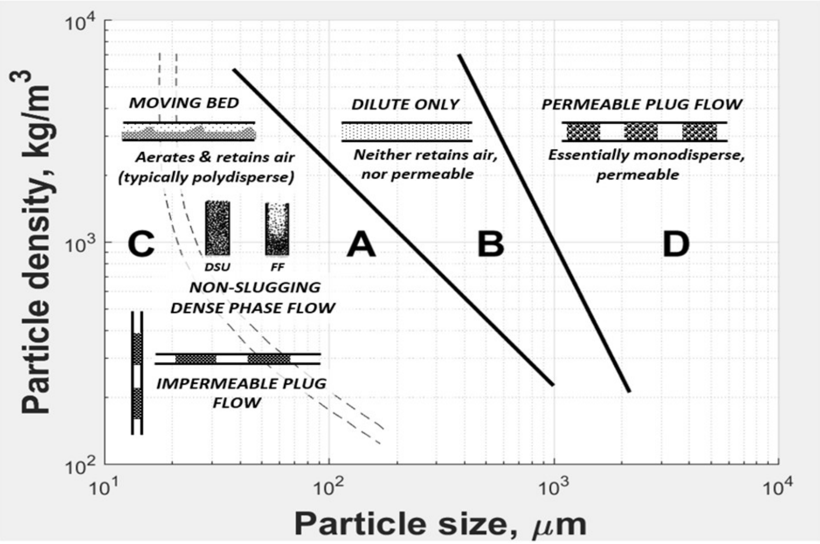

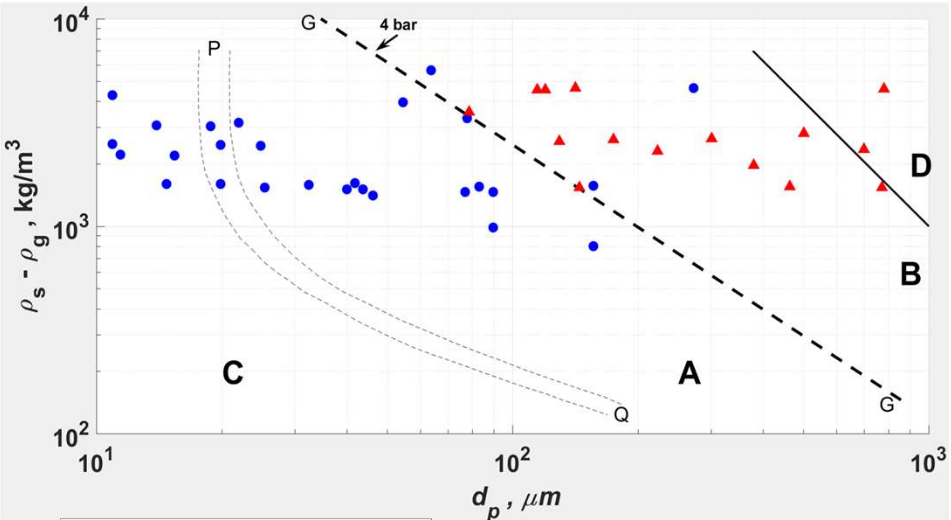

● FDC ▲ Dilute phase only

Geldart A-B boundary at 4 bar per Grace (1986)
Conveying mode data from Jones and Williams (2008)

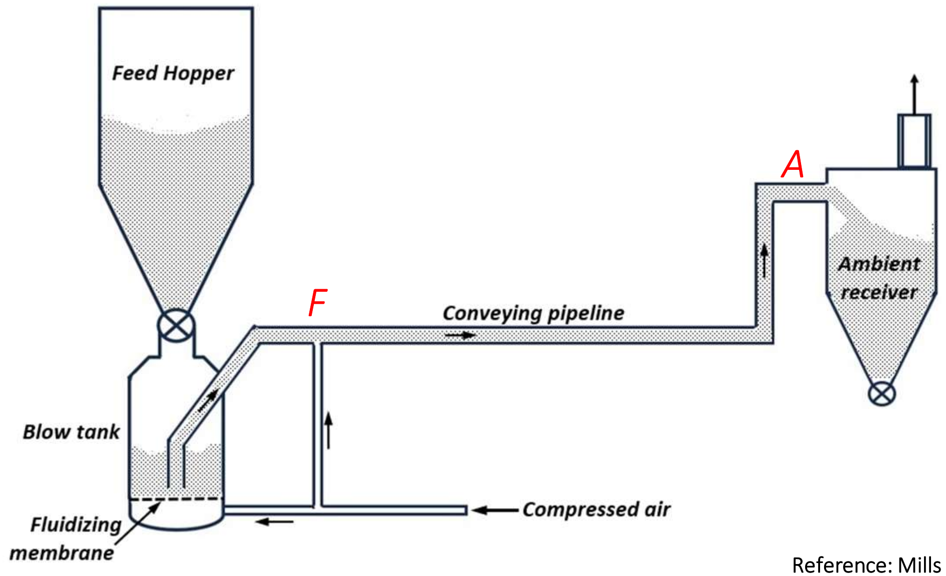

Reference: Mills (2004)

Typical Fluidized Dense Phase Conveying System and Operating Conditions

Description		Feed zone (*F*)	Ambient Receiver (*A*)
Maximum Solids loading (m)	kg / kg of air	150 - 300	
Maximum Solids flux (G_s)	kg / m^2 s	1000 - 3000	
Pressure	bar	2.5 - 4.0	Ambient
Solids volume fraction (ε_s)	-	0.09 - 0.38	0.03 - 0.18
Superficial gas velocity (V_g)	m / s	3 - 4	9 - 12
Conveying Pipeline	-	Typically, up to a few hundred meters long, > 80 % horizontal, with several bends	

Vertical up flow phase map

Vertical upflow patterns of Geldart A powders

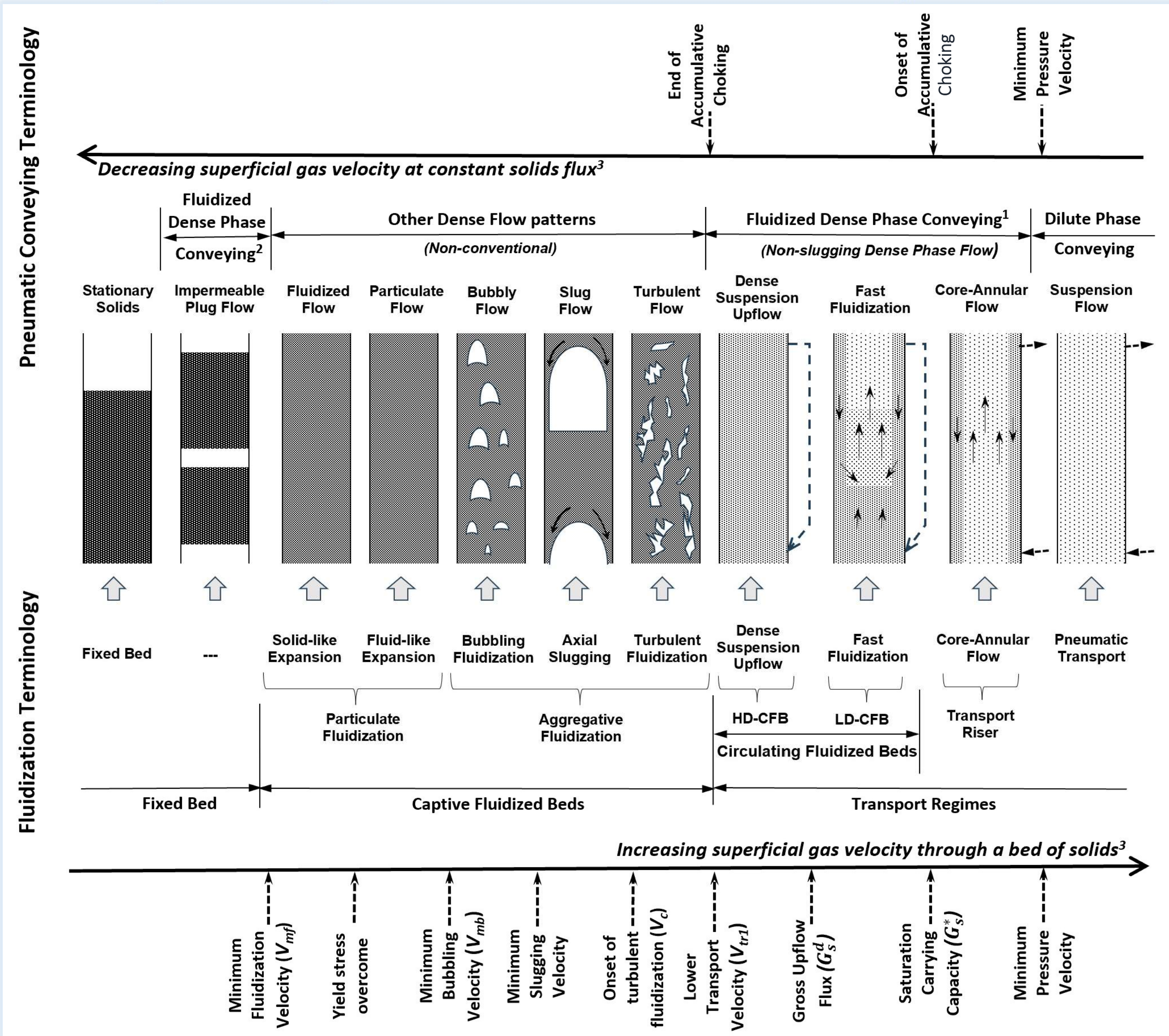

Notes:

1. For 'slightly cohesive' powders (HR < 1.25) which are easy to aerate and under well aerated conditions. They show clear pressure minima in the conveying characteristics.
2. Impermeable plug flow may occur with slightly cohesive powders (HR < 1.25) in conventional FDC systems under inadequate aeration; sustained operation may require a suitable feeder.
3. **Core-Annular Flow (CAF), Fast Fluidization (FF) and Dense Suspension Upflow (DSU) may occur at a same V_g but at different G_s: CAF at $G_s < G_s^*$, FF (LD-CFB) at $G_s^* < G_s < G_s^d$ and DSU (HD-CFB) at $G_s > G_s^d$**

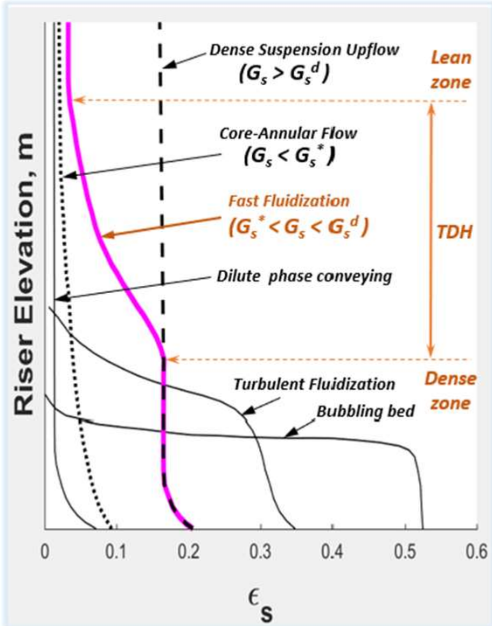

Axial ε_s profiles

(Adapted from Kunii and Levenspiel, 1991 to include CAF and DSU)

Referenes for the flow patterns: Bi et al., 2000, 1993; Bi and Grace, 1999; Cocco et al., 2010; Kalman and Rawat, 2020; Klinzing et al., 2010; Kunii and Levenspiel, 1991; Liu et al., 1996; Loezos et al., 2002; Mills, 2004; Rabinovich and Kalman, 2011; Valverde, 2013; Wirth, 1988; Yerushalmi and Avidan, 1985

Vertical Up Flow Phase Map of Wirth adapted to FDC of Geldart A powders

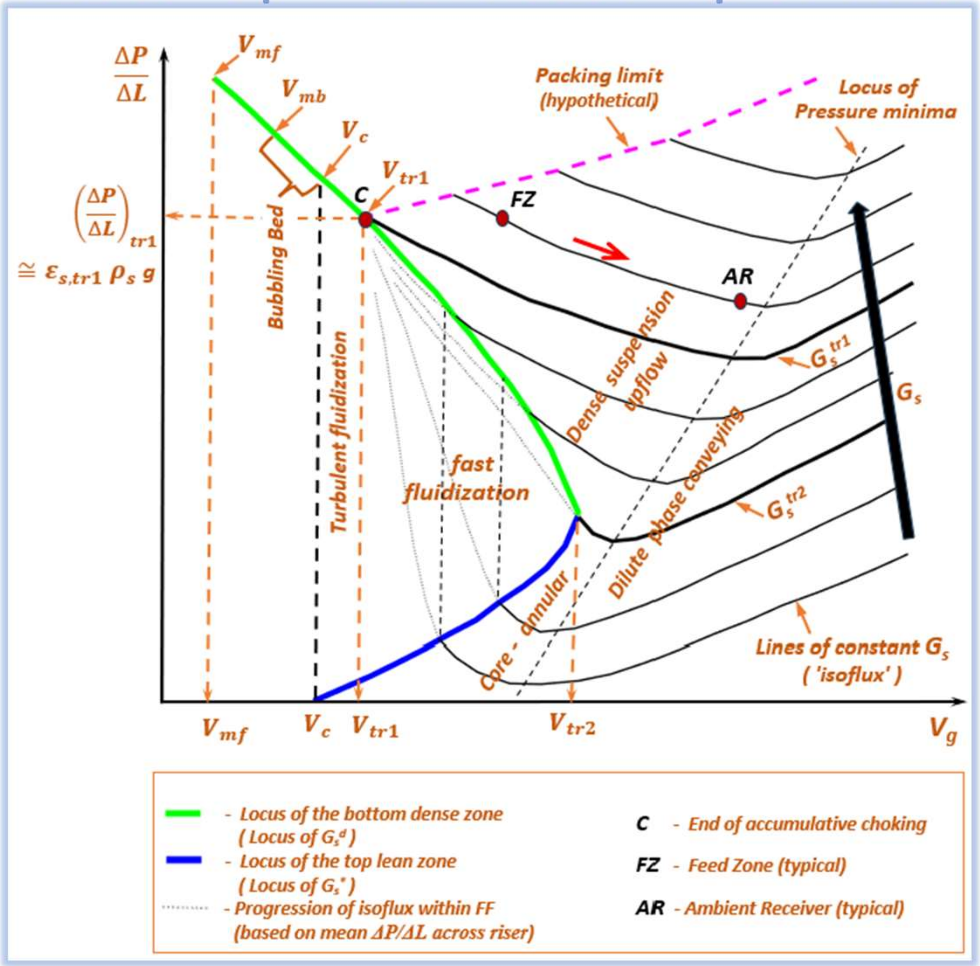

$\Delta P/\Delta L$ – Pressure gradient; V_g – Superficial gas velocity; V_{mf} – Minimum fluidization velocity; V_{mb} – Minimum bubbling velocity; V_c – Onset of turbulent fluidization; V_{tr1}– Lower transport velocity, V_{tr2} – Upper transport velocity; G_s– Solids flux; G_s^* – Saturation carrying capacity; G_s^d – Gross upflow flux; $G_{s,tr2}$ – G_s corresponding to V_{tr2}, the threshold G_s for Dense Suspension Upflow; $G_{s,tr1}$ – G_s corresponding to V_{tr1}

Phase map of Wirth adapted for Geldart A powders

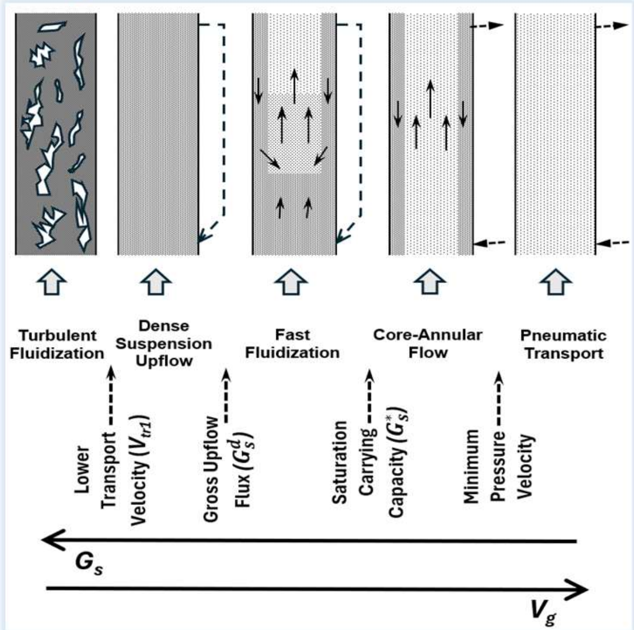

- DSU and its transition boundaries are not broadly accepted [Grace et al.(1999); Breault(2023)].
- Different criteria have been proposed for the FF – DSU transition:
  1. Disappearance of the s-shaped axial ε_s profile. [Li and Kwauk (1980)]
  2. G_s at which net upflow is attained in the dense annular region [Kim et al. (2004)]
- Recent experiment of Wang et al.(2022) (Fig.3 & 11) suggests that the FF – DSU transition (defined in this project as the disappearance of the s-shaped axial ε_s profile) only occurs at gross upflow of solids in the entire riser (G_s^d), with little backmixing. However, this requires validation, as the solids entering (although fluidized) at a lower velocity at the riser bottom could have formed a denser zone.
- The locus of pressure minima is broadly accepted as the boundary with dilute phase conveying at low G_s (typically $\varepsilon_s \cong$ 0.02), however, its suitability for the high G_s of FDC requires validation.
- Resolved experimental data for the packing limit is scarce, and hence an hypothetical limit is proposed, considering that the dense locus (green) at $V_g < V_{tr1}$ is unique and independent of G_s, and that the limit essentially lies where the available $\Delta P/\Delta L$ balances the dominant losses under the dense conditions, static head of solids and drag.

- DSU and its transition boundaries are not broadly accepted [Grace et al.(1999); Breault(2023)].
- Different criteria have been proposed for the FF – DSU transition :
  1. Disappearance of the s-shaped axial $\boldsymbol{\varepsilon_s}$profile. [Li and Kwauk (1980)]
  2. $\boldsymbol{G_s}$ at which net upflow is attained in the dense annular region [Kim et al. (2004)]
- Recent experiment of Wang et al.(2022) (Fig.3 & 11) suggests that the FF – DSU transition (defined in this project as the disappearance of the s-shaped axial $\boldsymbol{\varepsilon_s}$profile) only occurs at gross upflow of solids in the entire riser ($\boldsymbol{G_s^d}$), with little backmixing. However, this requires validation, as the solids entering (although fluidized) at a lower velocity at the riser bottom could have formed a denser zone.
- The locus of pressure minima is broadly accepted as the boundary with dilute phase conveying at low $\boldsymbol{G_s}$ (typically $\boldsymbol{\varepsilon_s} \cong$ 0.02), however, its suitability for the high $\boldsymbol{G_s}$ of FDC requires validation.
- Resolved experimental data for the packing limit is scarce, and hence an hypothetical limit is proposed, considering that the dense locus (green) at $V_g < V_{tr1}$ is unique and independent of G_s, and that the limit essentially lies where the available $\Delta P/\Delta L$ balances the dominant losses under the dense conditions, static head of solids and drag.

References for the phase map: Adapted from Wirth (1988), with inputs from Bi et al., 2000; Breault, 2023; Cocco et al., 2010; Kim et al., 2004; Li and Kwauk, 1980; Monazam and Shadle, 2011; Wang et al., 2022; Yerushalmi and Avidan, 1985

Proposed correlation for the Upper transport velocity (V_{tr2})

Proposed (provisional) correlation for the Upper transport velocity (V_{tr2})

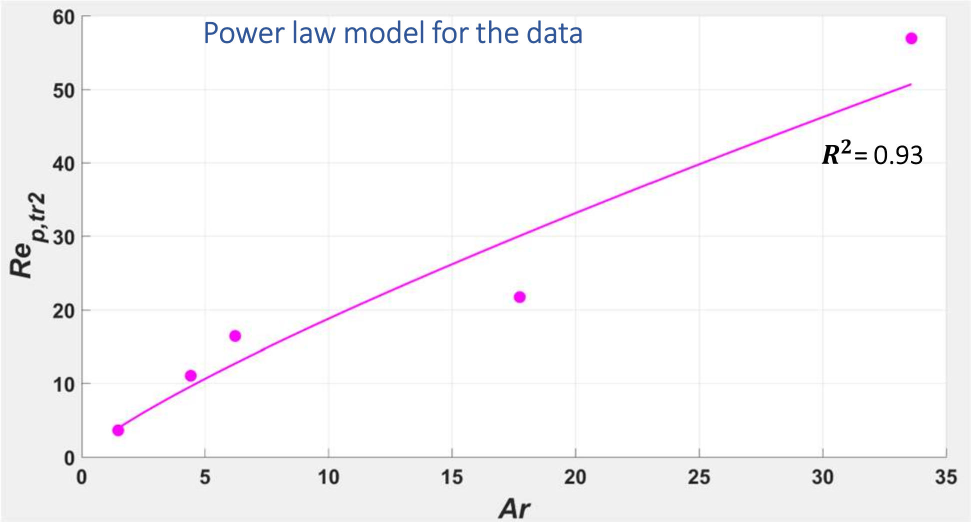

Note: A linear model (R^2 = 0.94) or an exponential model (R^2 = 0.97) may offer a better fit; however, $Re_p - Ar$ correlations generally follow power law and further rigour is not attempted considering the uncertainty in the data.

Correlation of Monazam & Shadle (2011):

Based on indirect measurement of V_{tr2} by column emptying times of solids (4 samples) that (tend to) group B.

$$Re_{p,tr2} = 3.118\, Ar^{0.487} \quad [1]$$

Proposed (provisional) correlation:

Based on 5 (sketchy) data points reported in the literature, for solids that clearly classify as group A, by direct measurement of V_{tr2} in CFB experiments at ambient conditions.

$$Re_{p,tr2} = 3.00\, Ar^{0.80} \quad [2]$$

Provisional, considering the recognized uncertainties in the data, and as the dependence on riser diameter (D) and fraction of fines (P_{45}) are not incorporated. However, it sufficiently demonstrates that V_{tr2} is significantly higher than predicted hitherto.

V_{tr2} data from literature for Geldart A powders

Powder	d_p μm	ρ_s kg/m³	P_{45}	D m	L m	L/D	Ar	V_{tr2} (Reported), m/s: Reported	V_{tr2} (Reported), m/s: Used	$Re_{p,tr2}$	V_{tr2} (Predicted), m/s: Per [1]	V_{tr2} (Predicted), m/s: Per [2]	Reference
Catalyst	(30)	(1500)	Not reported	0.19	11.5	61	1.48	1.8	1.8	3.62	1.88	2.04	(Wirth, 1988) (Fig.7, pp.15)
FCC catalyst	55	729	Not reported	0.05	5.0	100	4.42	2.5 & 3.5	3.0	11.05	1.74	2.68	(Mori et al., 1992)
HFZ-20	49	1450	~ 0.32	0.15	8.5	56	6.22	> 4.1	5.0	16.41	2.31	3.95	(Yerushalmi and Avidan, 1985) (Fig.7.21 b, pp.259)
Alumina (fine)	54	3160	Not reported	0.09	8.0	89	17.75	> 5.0	6.0	21.70	3.50	8.29	(Li and Kwauk, 1980) (Fig.2, pp.540)
FCC catalyst	85	1500	~ 0.10	0.08	18.0	225	33.60	> 9.0	10.0	56.93	3.03	8.77	(Wang et al., 2022) (Fig.11 - II, pp.8)

Proposed (provisional) correlation for the Upper transport velocity (V_{tr2})

Recognized uncertainties in the V_{tr2} data points:

- Wirth (1988) had only reported V_t for the 'finely divided catalyst' powder; d_p has been estimated considering a ρ_s of 1500 kg/m^3.
- Mori et al. (1992) had reported two different values for V_{tr2}, which is rather unique, affected by system design and operation; average of the values is used.
- Yerushalmi and Avidan (1985) had reported data for the HFZ-20 powder only up to a V_g of 4.1 m/s, at which the axial S-shaped ε_s profile is still very prominent; a V_{tr2} of 5 m/s is used.
- Li and Kwauk (1980) had reported data for the fine alumina only up to a V_g of ~ 5.0 m/s, and had projected a V_{tr2} of ~ 6.0 m/s.
- Wang et al. (2022) data for the FCC catalyst is limited to 9.0 m/s, at which they had approached (but not attained) V_{tr2} ; a V_{tr2} of 10 m/s is used.

Differences in flow behaviour of Geldart A and B powders in CFB:

- Dependence of both V_{tr1} and V_{tr2} on G_s^* is intuitive.
- Experiments have shown that G_s^* increases with D for Geldart A but decreases for Geldart B; and in fact Breault et al. [Breault and Weber(2021) ; Breault et al.(2021)] have proposed separate correlations for groups A and B.
- While ε_s^* is ~ 0.01 for Geldart B, it increases with decreasing d_p and/or ρ_s to ~ 0.03 for Geldart A. [Bi et al. (1995)]
- V_{tr1} Is a higher multiple of V_t for Geldart A than for Geldart B, also increasing with decreasing d_p and/or ρ_s. [Bi et al. (1995)]

Dependence of V_{tr2} on riser diameter (D):

- Wang et al., (2022) approached (but not attained) V_{tr2} at a $V_g$of 9 m/s with a FCC powder (d_p (85 µm), ρ_s (1500 kg/m^3) and P_{45} (~10 wt.%)) in a riser of D = 0.08 m.
- However, Issangya et al., (2023) observed very prominent axial S-shaped ε_s profile at a V_g of 12.2 m/s (G_s = 285 – 690 kg/m^{2}s) in a riser of D = 0.303 m, also with a FCC powder of similar d_p (79 µm), ρ_s (1490 kg/m^3) and P_{45} (~8 wt.%).

Proposed (provisional) correlation for the Upper transport velocity (V_{tr2})

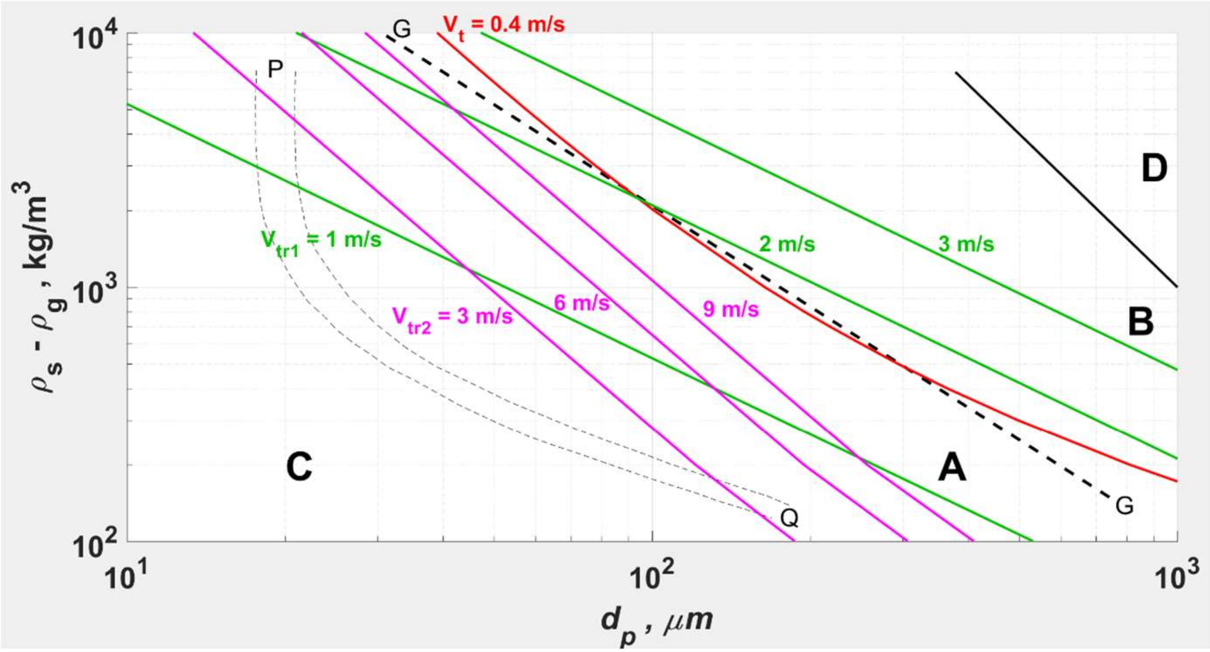

V_t , V_{tr1} and V_{tr2} at ambient pressure relative to A-B boundary

V_t per Haider and Levenspiel (cited in Kunii & Levenspiel (1991))
V_{tr1} per the correlation of Bi et al. (1995)
V_{tr2} per the proposed (provisional) correlation.

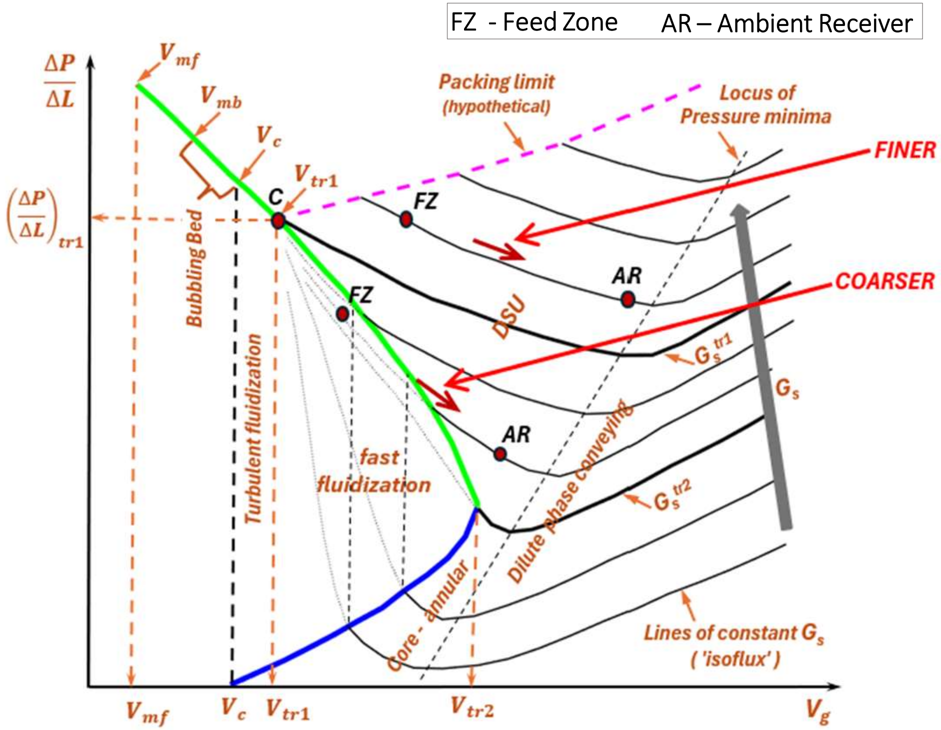

Operating regions of FDC for finer and coarser group A powders

Published experimental data suggests that FDC for finer Geldart A powders, wherein the window of FF is narrow due to low V_{tr2} (and G_s^{tr2}), operates at $G_s > G_s^{tr1}$. With increasing particle size (d_p) and / or density (ρ_s), as the window of FF expands due to increasing V_{tr2} , the operation shifts to $G_s^{tr2} < G_s < G_s^{tr1}$, or even within the FF zone at $G_s < G_s^{tr2}$.

Validation by Eulerian modelling with MFiX-TFM

- Powder characteristics
- Modelling options
- Challenges in model validation
- FF – DSU boundary at gross upflow
- DSU – dilute phase boundary
- Packing limit

Powder Characteristics

Characteristics of the (hypothetical) powder at ambient conditions

Particle diameter	d_p	μm	70	**Monodisperse**
Particle density	ρ_s	Kg/m³	1400	
Archimedes number	*Ar*		17.5	
Void fraction loose packed	$\varepsilon_{s,max}$		0.60	Maximum packing limit
Interparticle restitution	*c_e*		0.95	Used for simulations
Particle – wall restitution	*e_w*		0.89	Foerster et al.(1994), Drake(1991), (6mm cellulose acetate spheres)
Angle of wall friction	*Phi_w*	°	11.86	
Angle of internal friction	*Phi*	°	30	McKeen & Pugsley (2003)
Terminal settling velocity	V_t	m / s	0.186	**Kunii & Levenspiel (1991)**
Min. fluidization velocity	V_{mf}	m / s	0.004	
Min. bubbling velocity	V_{mb}	m / s	0.012	
Lower transport velocity	V_{tr1}	m / s	1.4	**Bi et al. (1995)**
Upper transport velocity	V_{tr2}	m / s	6.3	**Proposed (provisional) correlation**

Particles do not agglomerate or deform permanently; no electrostatic effects or liquid bridges.

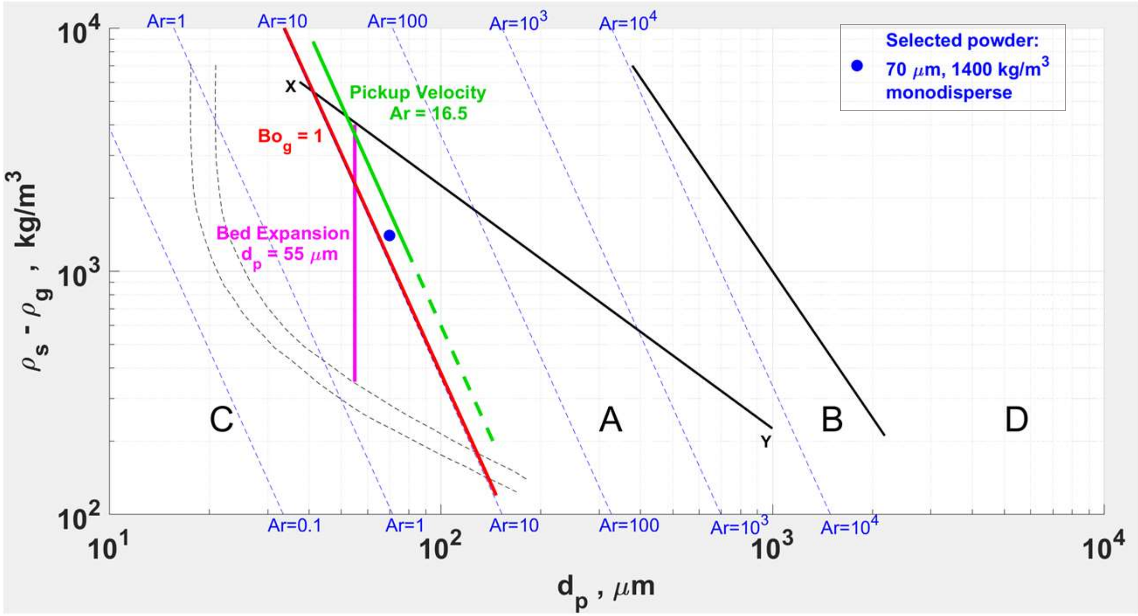

Threshold for dominant van der Waals forces over gravity

Different criteria have been proposed for dominant van der Waals forces over gravity:

(1) d_p= 55 μm, based on bed expansion [Loezos et al.(2002), Wang et al.(2011)]

(2) Bo_g (granular bond number) = 1 [Valverde(2013)]

(3) Ar = 16.5, based on pickup velocity [Kalman et al.(2005)]

Cohesion model is not considered essential for the monodisperse powder selected.

Modelling options – Simulation conditions

Modelling options are largely in line with Balasubramanian et al.(2023)

Description	Nominal	Alternate
MFiX version	22.3.1	22.3.1
Viscous stress model	Simonin	Lun et al.(1984)
Turbulence model	k-epsilon	--
Frictional stress model	Princeton	Princeton
Inlet & Outlet BC	MI & PO	MI & PO
Wall BC for gas phase	NSW (Wall functions)	NSW
Wall BC for solids phase	FSW / JJ-Mod	FSW
Drag model	Di Felice	Di Felice

Geometry and numerics

Description			Nominal grid	Fine grid
Riser (pipeline) diameter	D	m	0.04	0.04
Riser (pipeline) length	L	m	10.0	9.999
Grid			20 x 5000	40 x 9999
Cell size		m	0.002	0.001
Cell size in particle diameters			29	14
Maximum time step		s	3×10^{-5}	1×10^{-5}
Parallel processing			DMP (1-8-1)	DMP (1-16-1)
Discretization			Superbee	
Tolerances			Default	

Cartesian 2D

(Reproduced from Balasubramanian et al. (2023))

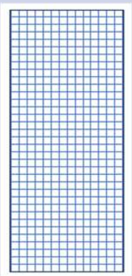

Advantages:

Matches the wall profile (although in 2D).

Qualitatively well predicts bed expansion, bubble rise, core-annular flow, clusters and streamers, etc.

Lower computational cost for long pipe models (e.g., S-shaped profile).

Offers rigorous wall BC.

Disadvantages:

Does not capture the inherent 3D nature of gas-solids flow.

Numerical predictions can be affected by asymmetric flows, e.g., inlet and outlet configurations. (Li et al. 2014-I)

May not simultaneously predict axial pressure profile and radial voidage accurately. (Li et al. 2014-II)

Optimum underrelaxation factors that prevent backflow with pressure outlet BC

(Reproduced from Balasubramanian et al. (2023))

For 2D Cartesian grid simulations #				
Under relaxation factor		Default	Selected	Remarks
UR_FAC(1)	Gas pressure	0.8	0.8	Improves stability
UR_FAC(2)	EP_s	0.5	1.0	
UR_FAC(3&5)	U&W-Momentums	0.5	0.5	Improves stability
UR_FAC(4)	V-Momentums	0.5	1.0	Set at 1.0 to avoid backflow at no / low solids loadings
UR_FAC(8)	Granular temperature	0.5	0.5	~ 1 in 3 runs diverges without underrelaxation
UR_FAC(9)	k-e	0.8	1.0	Set at 1.0 to avoid backflow at no / low solids loadings
UR_F_GS	Drag	1.0	0.0	Improves stability at ~ 3% increase in wall time

- May not be suitable for other coordinate systems or simulation conditions

Reproduced from Balasubramanian et al. (2023)

Modelling options – Model scheme

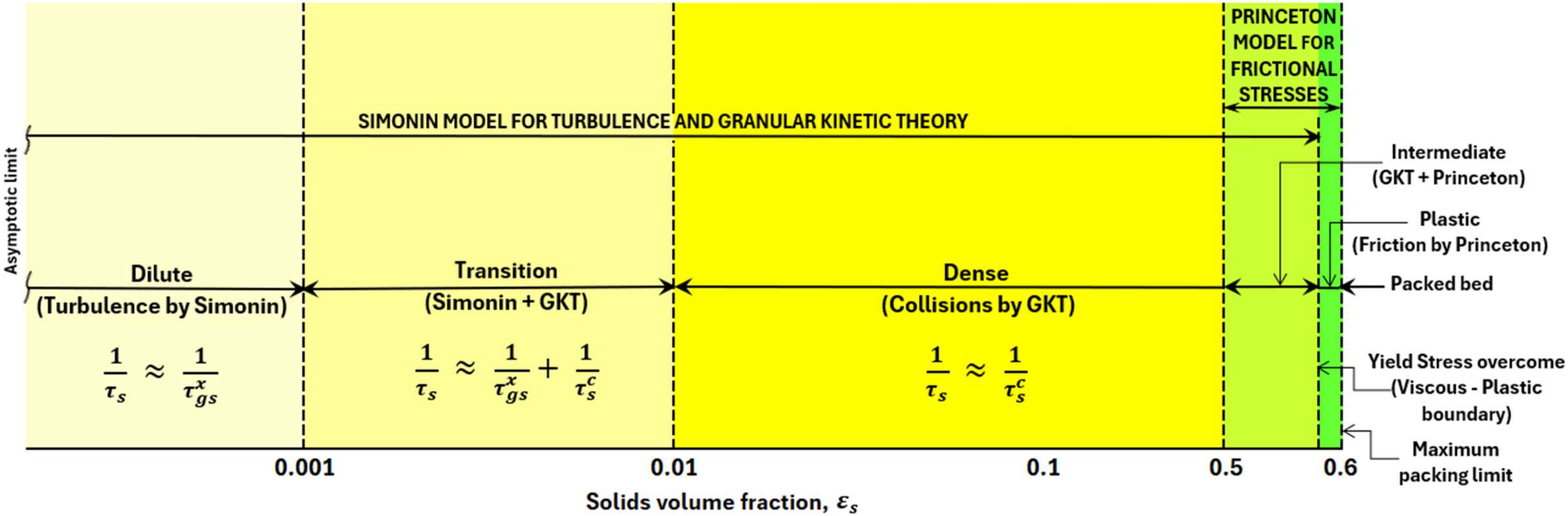

Simonin viscous stress model covers dilute turbulent through to the dense limit of viscous regime by a harmonic mean of collisional and particle relaxation time scales; Simonin's turbulence model and the GKT are recovered at the dilute and dense limits, respectively.

τ_s **- Dissipation time scale, s**

τ_{gs}^x **- Particle relaxation time, s**

τ_s^c **- Collisional time scale, s**

Reference: Balzer et al.(1996) Benyahia et al.(2005) & (2007), Srivastava & Sundaresan (2003)

➢ Challenges in model validation – Lower ε_s at the walls at higher G_s

20 x 5000 x 1, V_g = 3 m/s, Simonin, JJ-Mod, c_e = 0.87, e_w = 0.89

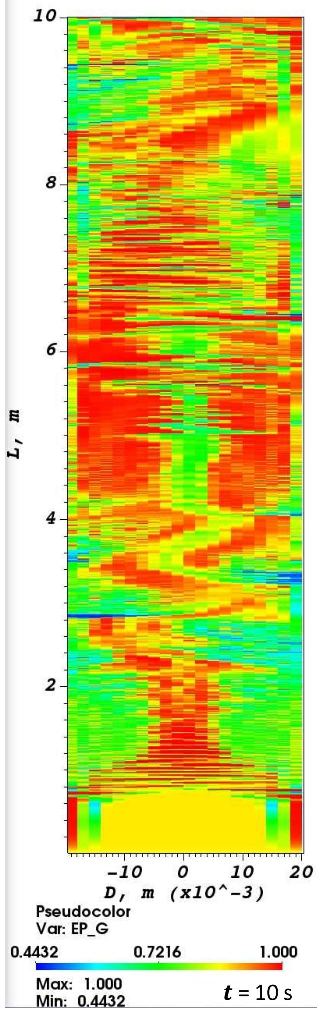

t = 10 s

G_s = 500 kg/m²s

Run VDU004

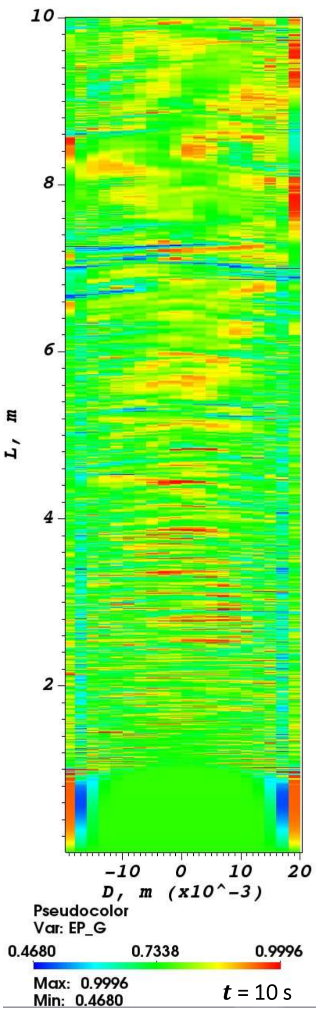

t = 10 s

G_s = 1000 kg/m²s

Run VDU001

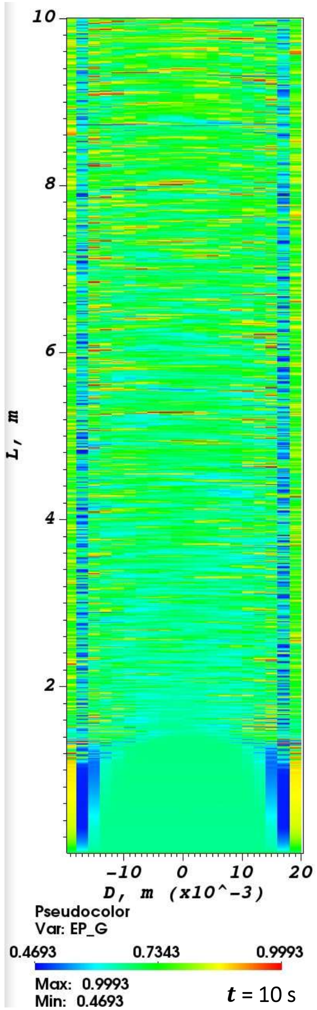

t = 10 s

G_s = 1500 kg/m²s

Run VDU002

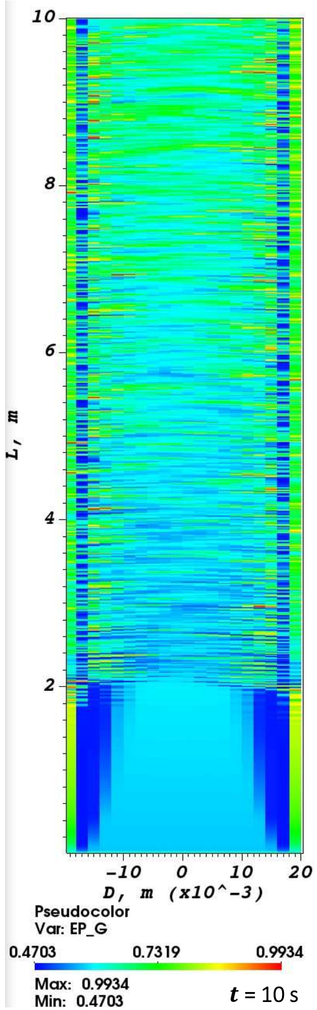

t = 10 s

G_s = 2000 kg/m²s

Run VDU003

Legend: At elevation 9m 7m 5m

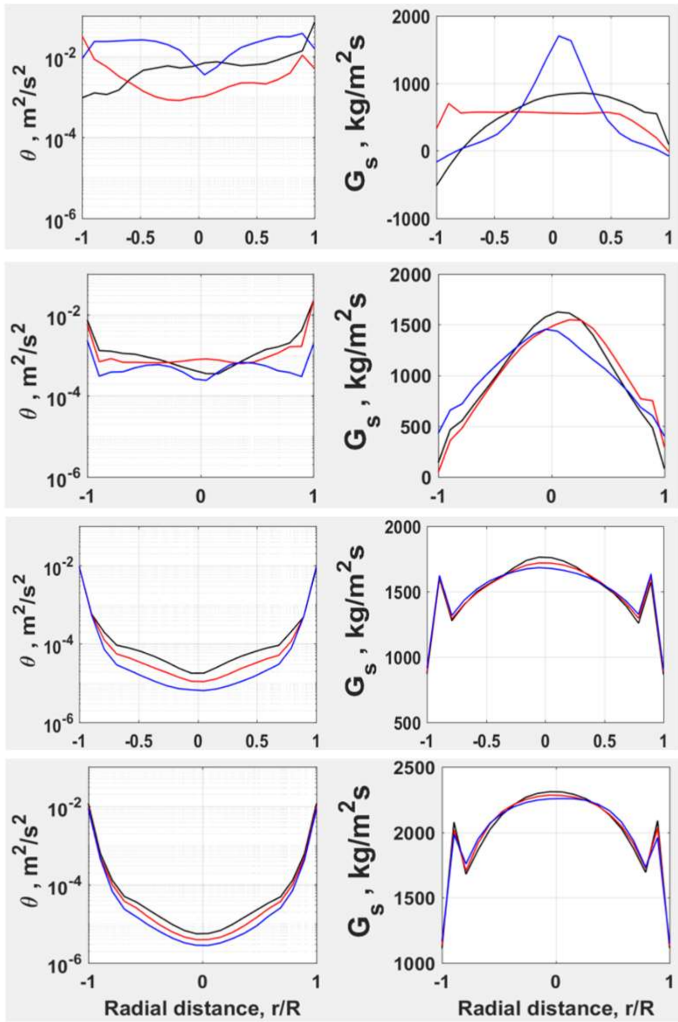

G_s = 500 kg/m²s

G_s = 1000 kg/m²s

G_s = 1500 kg/m²s

G_s = 2000 kg/m²s

- Solids displaced from wall at high G_s, apparently due to dissipation of θ in the bulk.
- Similar spike in G_s in the pre-wall region can be seen in the experimental data of PSRI: Fig.8 of Issangya et al.(2023) and Fig.26 of Cocco et al.(2010).

GCU Glasgow Caledonian University

➢ Challenges in model validation – Lower $\boldsymbol{\varepsilon_s}$ at the walls at higher $\boldsymbol{G_s}$

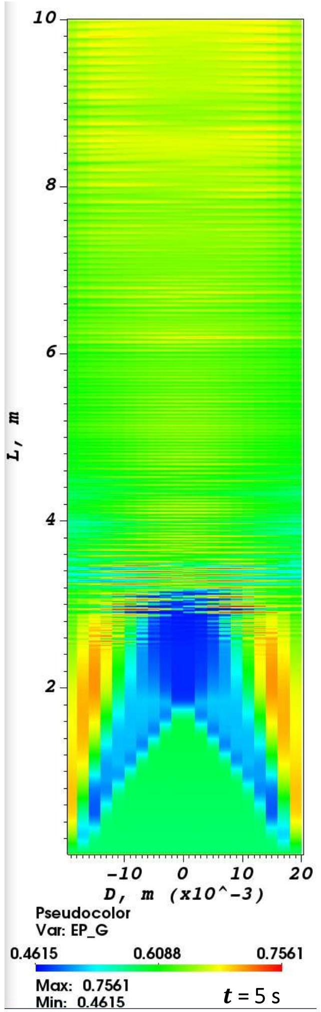

c_e = 1.00

Run VDU020

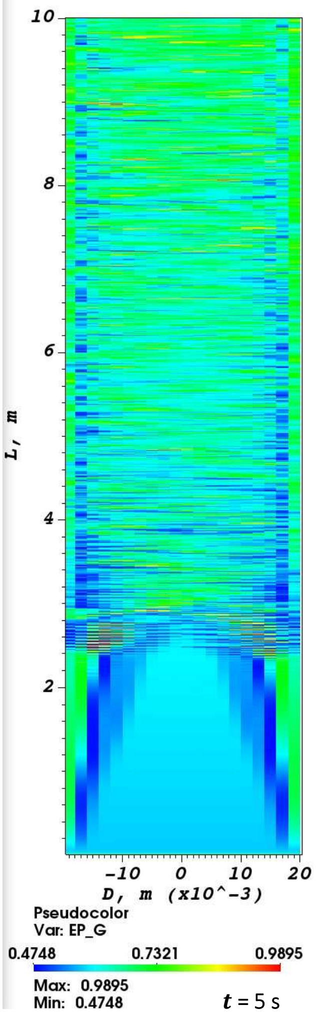

c_e = 0.99

Run VDU021

20 x 5000 x 1, V_g= 3 m/s, G_s=2000 kg/m²s, Simonin, FSW

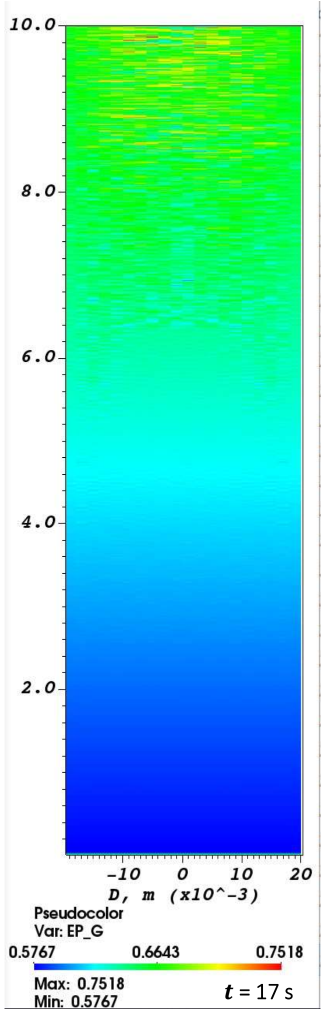

Lun et al. +FSW

(NSW for gss & no turbulence model)

Run VDU023

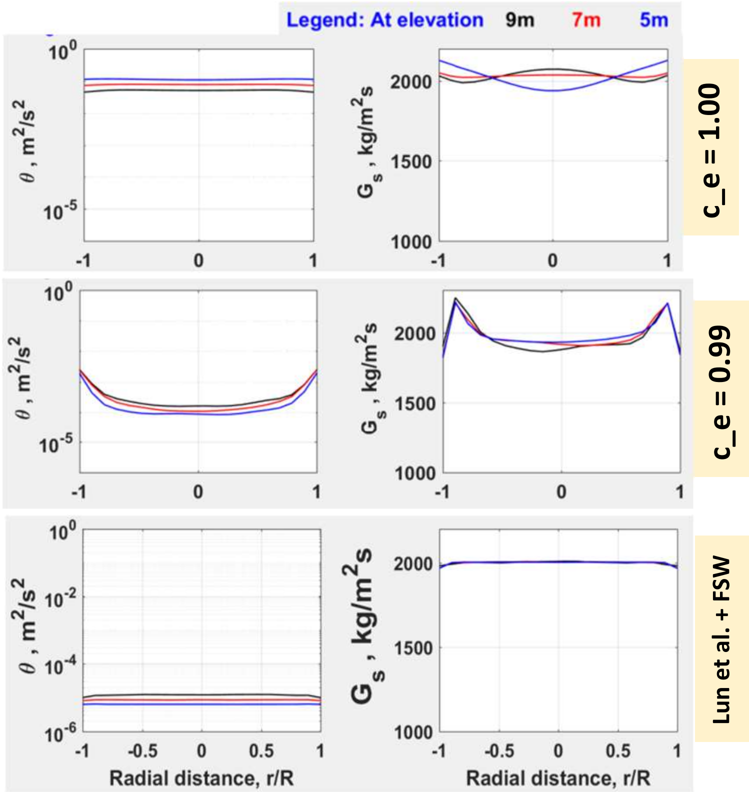

- Solids are not displaced from the wall with elastic particles but are even with c_e = 0.99 . This would similar to that reported in early TFM literature (e.g. Pita & Sundaresan, 1991).
- Solids are displaced from the wall with the following options too:
  - ✓ Simonin with FSW
  - ✓ Lun et al. with JJ-Mod
- Not due to turbulence wall functions:
  - ▪ No perceivable change when wall functions are turned off with Simonin + FSW.
  - ▪ No perceivable change when k-epsilon turbulence model is turned on with Lun et al. + FSW
- *Lun et al. with FSW gives smooth results, although with high dissipation of* $\boldsymbol{\theta}$ *in the bulk. Hence has been used for comparison runs.* (High inlet transition length with this option has been accounted for.)

➢ Challenges in model validation – Lower V_{slip} than reported in the literature

20 x 5000 x 1, V_g = 3 m/s, Simonin, FSW, c_e = 0.95, Di Felice

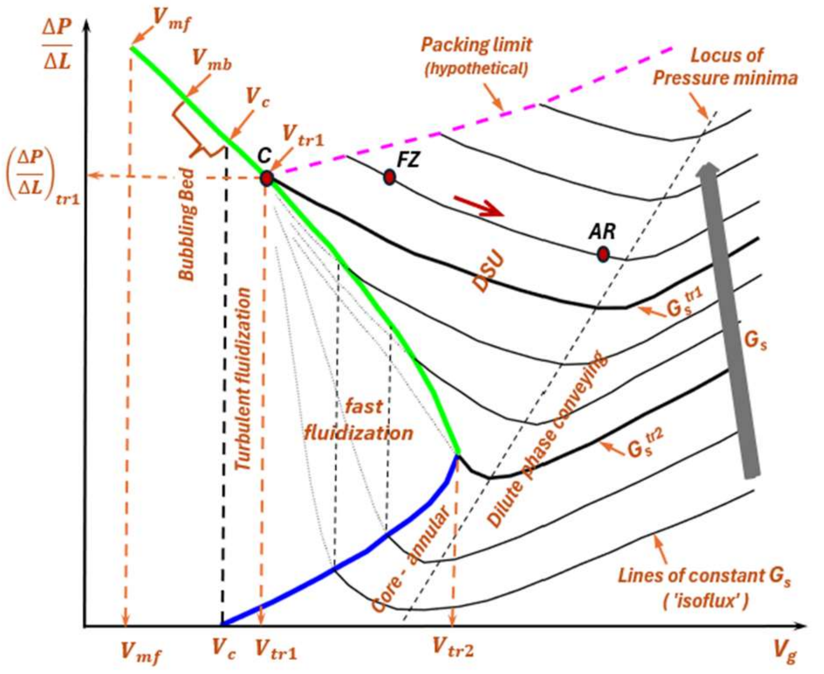

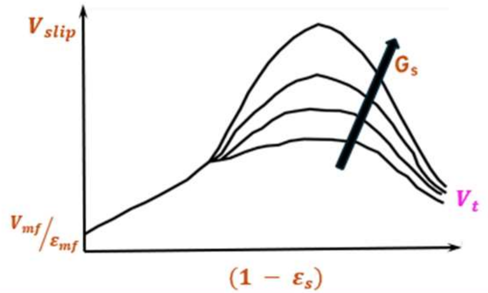

Slip velocity (V_{slip}) in CFBs

V_{slip} in FF is reported to be up to an order of magnitude higher than V_t; to increase with G_s; and even higher under dense upflow. However, the model predicts a steady decrease with G_s .

Yerushalmi & Cankurt (1979), Grace (2000), Benyahia & Sundaresan (2012)

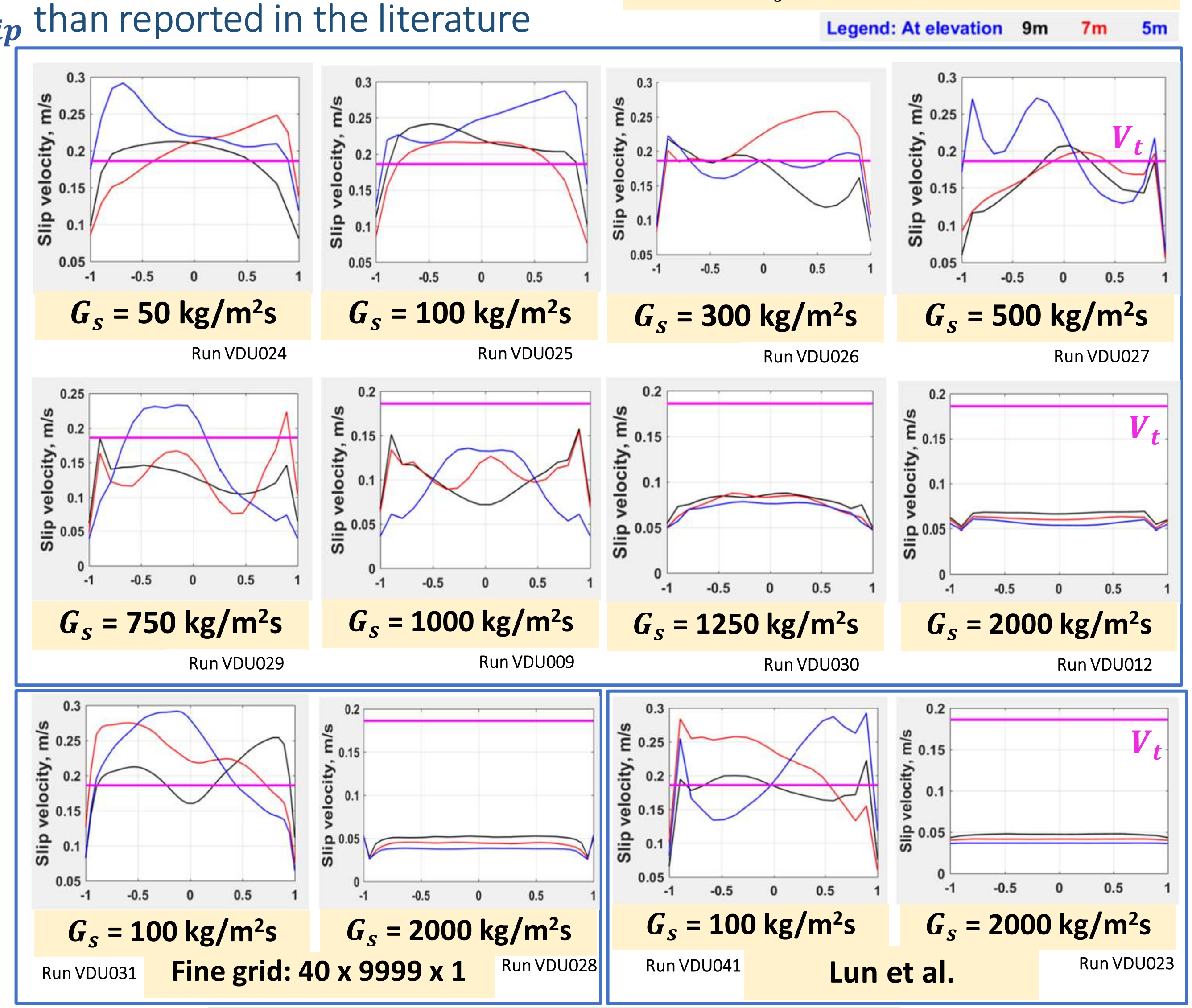

- Gidaspow blend drag model has not made any material difference either.

Validation by Eulerian modelling with MFiX-TFM

➢ Validation: FF – DSU boundary at gross up flow of solids

20 x 5000 x 1, V_g = 3 m/s, Simonin, FSW, c_e = 0.95, Di Felice

Legend: At elevation 9m 7m 5m

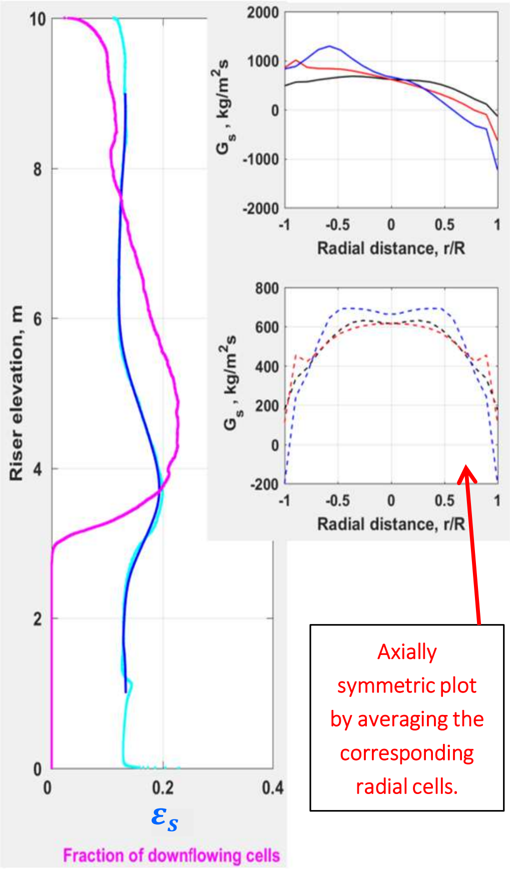

G_s = 500 kg/m²s

Run VDU027

Downflowing annulus

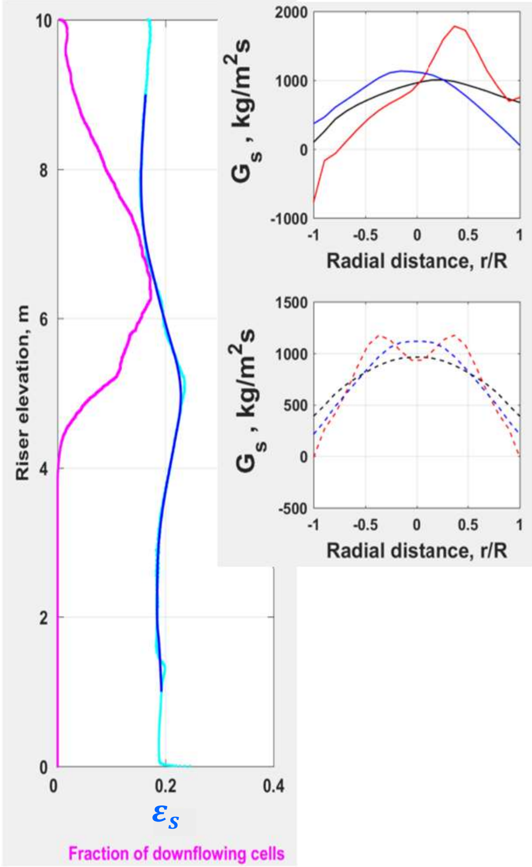

G_s = 750 kg/m²s

Run VDU029

Approaching net upflow

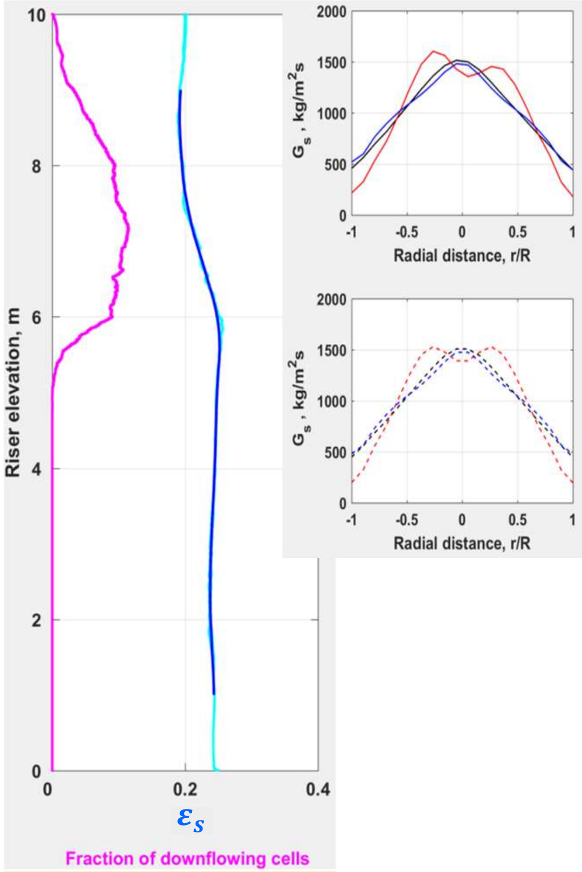

G_s = 1000 kg/m²s

Run VDU009

Net upflow

S-shaped axial ε_s profile clearly seen.

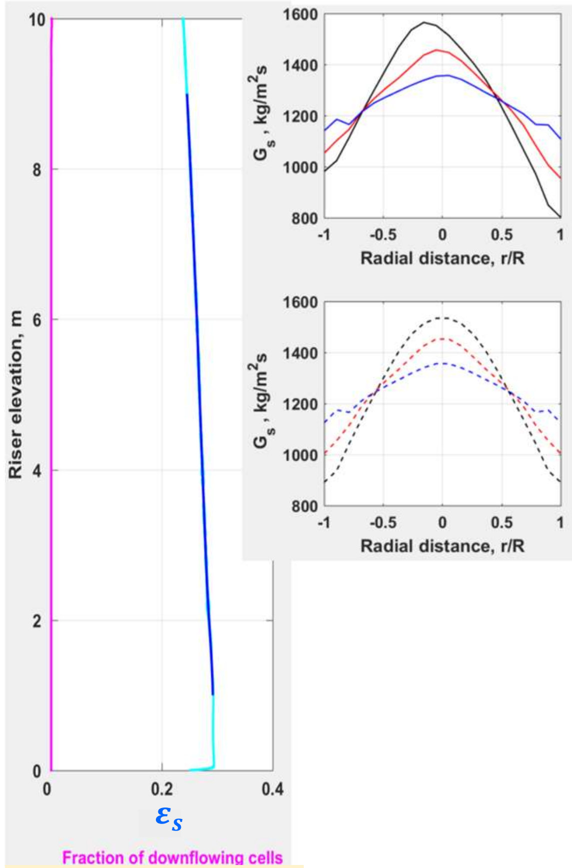

G_s = 1250 kg/m²s

Run VDU030

Gross upflow

S-shaped axial ε_s profile has disappeared.

➢ Validation: DSU – Dilute phase boundary and packing limit

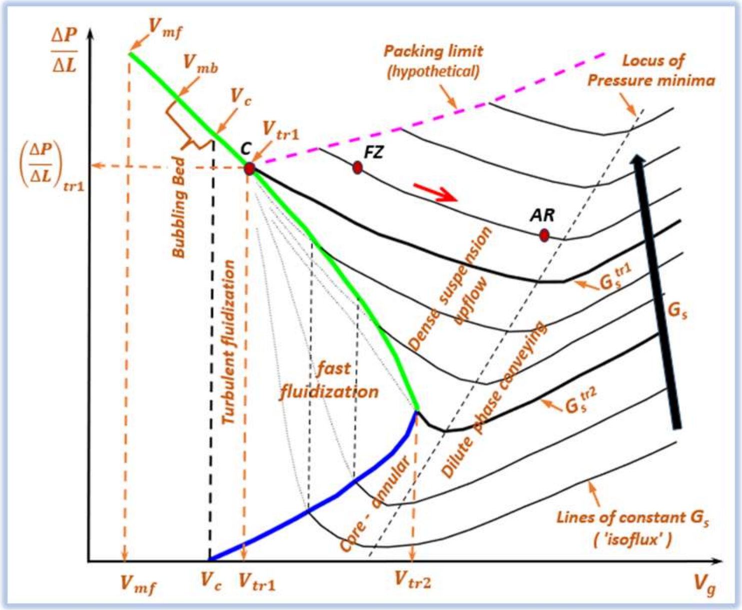

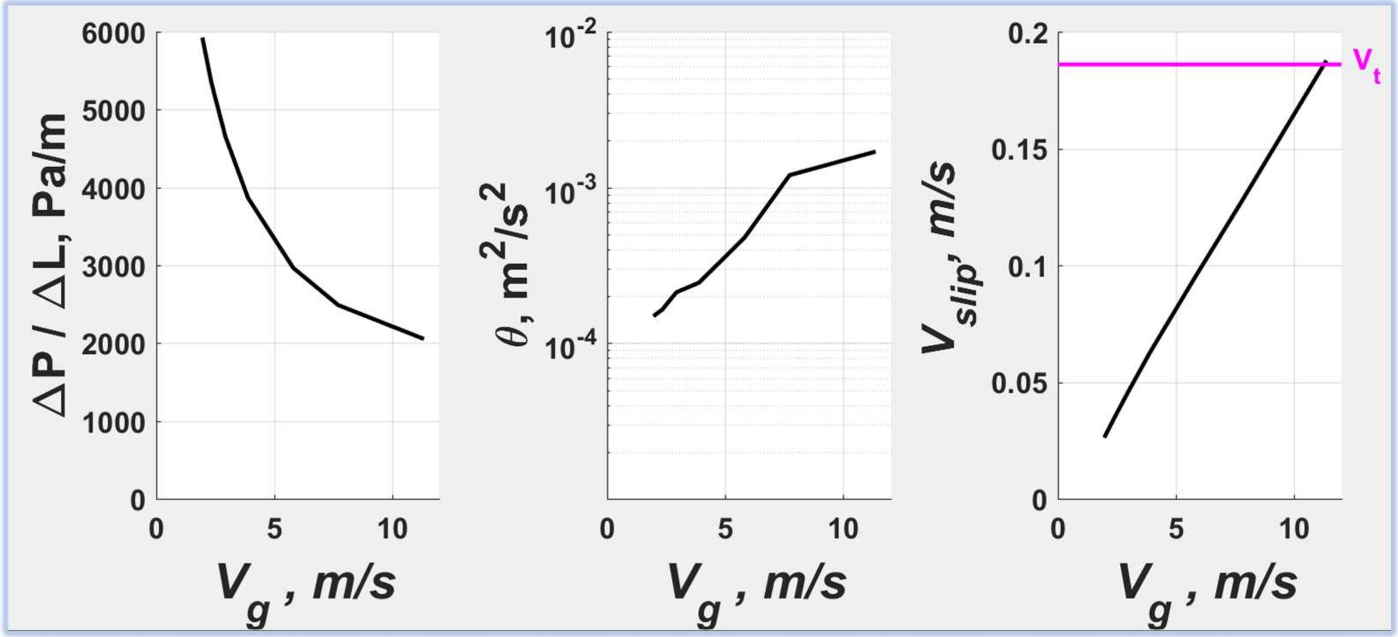

Solids flux = 2000 kg / m² s

Conditions at the feed zone:

V_g = 3 m/s at 4 bar

- For the conditions simulated, pressure minimum is not attained at the ambient receiver.
- Trends in granular temperature and slip velocity are probable aternate variables to perceive the transition.
- As precited by Granular Kinetic Theory, gravity dominates the pressure drop at the packing limit and drag is insignificant (due to the very low slip velocity).
- Contribution of other pressure losses (drag, etc.) increase from ~ 2% at the packing limit to > 20% at the ambient receiver.

Conclusions

- **Vertical upflow phase map of Wirth adapted to locate Fluidized Dense Phase Conveying of Geldart A powders. The map demarcates the boundaries of Dense Suspension Upflow with Fast Fluidization, dilute phase conveying and the packing limit.**

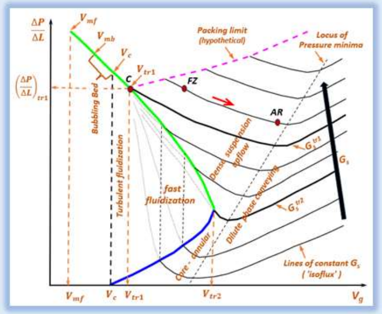

- **Proposed a provisional correlation for the Upper transport velocity (V_{tr2}) of group A powders, based on a limited (sketchy) data set, without accounting for its dependence on riser diameter (D) and fines fraction (P_{45}). The correlation sufficiently demonstrates that is significantly higher than hitherto predicted.**

$$Re_{p,tr2} = 3.00\ Ar^{0.80}$$

- **Highlighted the challenges faced in validating the MFiX-TFM model at high solids flux: low solids concentration near the wall and lower slip velocities than reported in CFB experiments.**
- **Demonstrated (based on the experimental results of Wang et al.(2022) and Eulerian modelling) that the transition from Fast Fluidization to Dense Suspension Upflow, defined as the disappearance of the S-shaped axial profile only occurs at gross upflow of solids in the entire riser.**
- **For the conditions simulated, transition to dilute phase conveying is not perceived at the ambient receiver based on the pressure gradient.**
- **Packing limit, as predicted by the Granular Kinetic Theory is largely due to static head of solids (as the predicted slip velocity is very low).**

Areas identified for further research:

1. **CFB experiments to measure V_{tr2} of group A powders, incorporating various riser diameters and fines fractions, for a robust correlation.**
2. **Validation of the TFM model for high solids flux applications.**

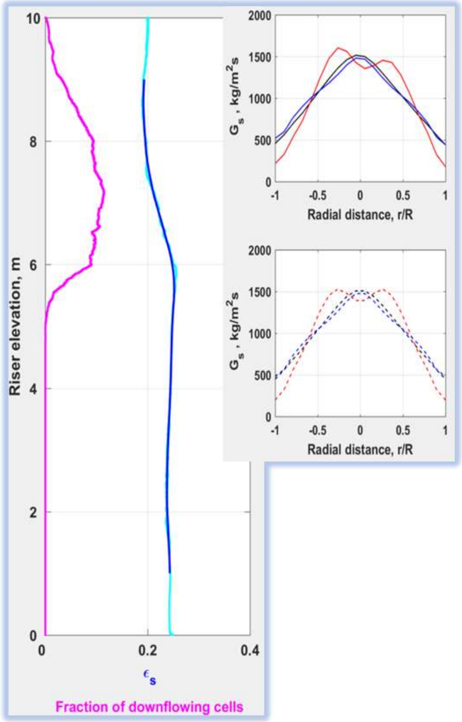

References

Balasubramanian, P., Cowell, A., McGlinchey, D., 2023. Modelling fluidized dense phase conveying of Geldart A powders with MFiX-TFM: A case study. Presented at the NETL 2023 Virtual Workshop on Multiphase Flow Science, National Energy Technology Laboratory, U.S. Department of Energy.

Balzer, G., Simonin, O., Boelle, A., Lavieville, J., 1996. A unifying modelling approach for the numerical prediction of dilute and dense gas– solid two phase flow, in: CFB5, 5th Int. Conf. on Circulating Fluidized Beds. Beijing, China.

Benyahia, S., Sundaresan, S., 2012. Do we need sub-grid scale corrections for both continuum and discrete gas-particle flow models? Powder Technology 220, 2–6. https://doi.org/10.1016/j.powtec.2011.10.052

Benyahia, S., Syamlal, M., O'Brien, T.J., 2007. Study of the ability of multiphase continuum models to predict core-annulus flow. AIChE Journal 53, 2549–2568. https://doi.org/10.1002/aic.11276

Benyahia, S., Syamlal, M., O'Brien, T.J., 2005. Evaluation of boundary conditions used to model dilute , turbulent gas / solids flows in a pipe. Powder Technology 156, 62–72. https://doi.org/10.1016/j.powtec.2005.04.002

Bi, H.T., Ellis, N., Abba, I.A., Grace, J.R., 2000. A state-of-the-art review of gas-solid turbulent fluidization. Chemical Engineering Science 55, 4789–4825.

Bi, H.T., Grace, J.R., 1999. Flow patterns in high-velocity fluidized beds and pneumatic conveying. The Canadian Journal of Chemical Engineering 77, 223–230. https://doi.org/10.1002/cjce.5450770206

Bi, H.T., Grace, J.R., Zhu, J., 1995. Regime transitions affecting gas-solids suspensions and fluidized beds. Chemical engineering research & design 73, 154–161.

Bi, H.T., Grace, J.R., Zhu, J.-X.X., 1993. Types of choking in vertical pneumatic systems. International Journal of Multiphase Flow 19, 1077–1092. https://doi.org/10.1016/0301-9322(93)90079-A

Breault, R.W., 2023. Scaling CFB risers: Maintaining microstructure dynamics. Powder Technology 415.

Breault, R.W., Weber, J., 2021. Saturation Carrying Capacity for Group A Particles in a Circulating Fluidized Bed. Energies (Basel) 14, 2809-.

Breault, R.W., Weber, J., Yang, J., 2021. Saturation carrying capacity Group B particles in a circulating fluidized bed. Powder technology 384, 442–451.

Cocco, R.A., Shaffer, F., Hays, R., Karri, S.B.R., Knowlton, T.M., 2010. Particle clusters in and above fluidized beds. Powder Technology 203, 3–11. https://doi.org/10.1016/j.powtec.2010.03.023

Di Felice, R., 1994. The voidage function for fluid-particle interaction systems. International journal of multiphase flow 20, 153–159.

Drake, T.G., 1991. Granular flow: physical experiments and their implications for microstructural theories. Journal of Fluid Mechanics 225, 121–152.

Foerster, S.F., Louge, M.Y., Chang, H., Allia, K., 1994. Measurements of the collision properties of small spheres. Physics of Fluids 6. https://doi.org/10.1063/1.868282

Grace, J.R., 2000. Reflections on turbulent fluidization and dense suspension upflow. Powder Technology 113, 242–248. https://doi.org/10.1016/S0032-5910(00)00307-7

Grace, J.R., 1986. Contacting modes and behaviour classification of gas—solid and other two-phase suspensions. The Canadian Journal of Chemical Engineering 64, 353–363.

Grace, J.R., Issangya, A.S., Bai, D., Bi, H., Zhu, J., 1999. Situating the high-density circulating fluidized bed. AIChE Journal 45, 2108–2116.

Issangya, A.S., Karri, S.B.R., Cocco, R.A., Knowlton, T., Chew, J.W., 2023. Solids flux profiles of Geldart Group A particles in high-velocity circulating fluidized bed risers. The Canadian Journal of Chemical Engineering 101, 256–268. https://doi.org/10.1002/cjce.24628

Jones, M.G., Williams, K.C., 2008. Predicting the mode of flow in pneumatic conveying systems - A review. Particuology 6, 289–300.

Kalman, H., Rawat, A., 2020. Flow regime chart for pneumatic conveying. Chemical Engineering Science 211.

Kalman, H., Satran, A., Meir, D., Rabinovich, E., 2005. Pickup (critical) velocity of particles. Powder Technology 160, 103–113. https://doi.org/10.1016/j.powtec.2005.08.009

Kim, S.W., Kirbas, G., Bi, H., Jim Lim, C., Grace, J.R., 2004. Flow behavior and regime transition in a high-density circulating fluidized bed riser. Chemical engineering science 59, 3955–3963.

Klinzing, G.E., Rizk, F., Marcus, R., Leung, L.S., 2010. Pneumatic Conveying of Solids A theoretical and practical approach, 3rd ed. Springer, Dordrecht.

Kunii, D., Levenspiel, O., 1991. Fluidization Engineering, 2nd ed. Butterworth-Heinemann.

Li, T., Gel, A., Pannala, S., Shahnam, M., Syamlal, M., 2014a. CFD simulations of circulating fluidized bed risers, part I: Grid study. Powder Technology 265, 2–12. https://doi.org/10.1016/j.powtec.2014.04.008

Li, T., Pannala, S., Shahnam, M., 2014b. CFD simulations of circulating fluidized bed risers, part II, evaluation of differences between 2D and 3D simulations. Powder Technology 254, 115–124. https://doi.org/10.1016/j.powtec.2014.04.007

Li, Y., Kwauk, M., 1980. The Dynamics of Fast Fluidization, in: Grace, J.R., Matsen, J.M. (Eds.), Fluidization. Springer US, Boston, MA, pp. 537–544. https://doi.org/10.1007/978-1-4684-1045-7_57

Liu, D., Kwauk, M., Li, H., 1996. Aggregative and particulate fluidization—The two extremes of a continuous spectrum. Chemical engineering science 51, 4045–4063.

Loezos, P.N., Costamagna, P., Sundaresan, S., 2002. The role of contact stresses and wall friction on fluidization. Chemical Engineering Science 57, 5123–5141. https://doi.org/10.1016/S0009-2509(02)00421-9

Massoudi, M., 2003. Constitutive relations for the interaction force in multicomponent particulate flows. International journal of non-linear mechanics 38, 313–336.

Mckeen, T., Pugsley, T., 2003. Simulation and experimental validation of a freely bubbling bed of FCC catalyst. Powder Technology 129, 139–152.

Mills, D., 2004. Pneumatic conveying design guide, 2nd ed. Elsevier, Butterworth Heinemann, Amsterdam.

Monazam, E.R., Shadle, L.J., 2011. Method and Prediction of Transition Velocities in a Circulating Fluidized Bed's Riser. Ind. Eng. Chem. Res. 50, 1921–1927. https://doi.org/10.1021/ie1013376

Mori, S., Liu, D., Kato, K., Kobayashi, E., 1992. Flow regimes and critical velocity in a circulating fluidized bed. Powder technology 70, 223–227.

Patro, P., Dash, S.K., 2014. Numerical simulation for hydrodynamic analysis and pressure drop prediction in horizontal gas-solid flows. Particulate Science and Technology 32, 94–103. https://doi.org/10.1080/02726351.2013.829543

Pita, J.A., Sundaresan, S., 1991. Gas-solid flow in vertical tubes. https://doi.org/10.1002/aic.690370706

Rabinovich, E., Kalman, H., 2011. Flow regime diagram for vertical pneumatic conveying and fluidized bed systems. Powder Technology 207, 119–133. https://doi.org/10.1016/j.powtec.2010.10.017

Srivastava, A., Sundaresan, S., 2003. Analysis of a frictional – kinetic model for gas – particle flow. Powder Technology 129, 72–85. https://doi.org/10.1016/S0032-5910(02)00132-8

Valverde, J.M.M., 2013. Fluidization of Fine Powders: Cohesive versus Dynamical Aggregation, 1st ed, Particle technology series. Springer Nature, Netherlands.

Wang, C., Su, X., Luo, M., Lan, X., Gao, J., Xu, C., Ye, M., Zhu, J., 2022. Flow characteristics in a pilot-scale circulating fluidized bed with high solids flux up to 1800 kg/m2 s. Powder Technology 405, 117542. https://doi.org/10.1016/j.powtec.2022.117542

Wang, J., van der Hoef, M.A., Kuipers, J.A.M., 2011. The role of scale resolution versus inter-particle cohesive forces in two-fluid modeling of bubbling fluidization of Geldart A particles. Chemical Engineering Science 66, 4229–4240. https://doi.org/10.1016/j.ces.2011.06.004

Wirth, K.-E., 1988. Axial pressure profile in Circulating Fluidized Beds. Chemical Engineering and Technology 11, 11–17.

Yerushalmi, J., Avidan, A., 1985. Chapter 7. High-Velocity Fluidization, in: Davidson, J.F., Clift, R., Harrison, D. (Eds.), Fluidization. Academic Press, Inc., Orlando, FL, United States.

Yerushalmi, J., Cankurt, N., 1979. Further studies of the regimes of fluidization. Powder Technology 24, 187–205.

Thank you!

I am grateful to Dr. Shahnam, MFiX team and the event organizers for accommodating my virtual participation.

I acknowledge the support received at the MFiX forum.

Please forward your comments to prabu.balasubramanian@gcu.ac.uk